Received March 1998
Revised November 1998
Accepted November 1998

Coupling heat conduction, radiation and convection in complex geometries

I. Rupp
SIMULOG, Guyancourt, France
C. Péniguel
EDF/DER LNH, Chatou, France

Keywords *Conjugate heat transfer, Heat transfer, Industrial applications, Numerical code, Radiation, Radiosity*

Abstract *In many industrial applications, convection radiation and conduction participate simultaneously to the heat transfers. A numerical approach able to cope with such problems has been developed. The code SYRTHES is tackling conduction and radiation (limited to non participating medium). Radiation is solved by a radiosity approach, and conduction by a finite element method. Accurate and efficient algorithms based on a mixing of analytical/numerical integration, and ray tracing techniques are used to compute the view factors. The fluid part is solved by CFD codes like ESTET (Finite volumes) or N3S (Finite elements). SYRTHES relies on an explicit numerical scheme to couple all the phenomena. No stability problems have been encountered. To provide further flexibility, the three phenomena are solved on three independent grids. All data transfers being automatically taken care of by SYRTHES. Illustrating applications are shown.*

Introduction

In many industrial applications, convection radiation and conduction participate simultaneously to the heat transfers. A numerical approach able to cope with such problems has been developed. Experimental approaches have been extensively used in the past, but they may become very costly when dealing with very hot temperature and pressure, and they often lack the flexibility needed when a parametric study is desired during the design phase. On the other hand, heat transfer analysis softwares are becoming quite promising to accurately calculate thermal phenomena and determine their consequences, especially since affordable and powerful computer facilities are available on the market.

The paper is focusing on the numerical technique used to tackle the problems. A first part will briefly present the equation which needs to be solved, then the paper focuses on the radiation problem. The view factors calculation in 2D (Cartesian and axisymmetrical cases) and in 3D is presented. The solver used to handle the radiosity system and the iterative technique used to couple the different phenomena are discussed. Finally, several examples illustrating some features of the code SYRTHES are included.

Equations to be solved

The conduction part

SYRTHES is a general purpose conduction code which solves the conduction equation by a finite element method on unstructured grids. All material

International Journal of Numerical Methods for Heat & Fluid Flow, Vol. 9 No. 3, 1999, pp. 240-256.

characteristics are allowed to vary with space and time. Anisotropy is handled as well as periodicity in several directions. Classical boundary conditions (prescribed temperature, flux, exchange conditions, contact resistance) are available. Efficient numerical methods makes possible the use of large meshes even on fairly small computers. Detailed informations on the conduction code can be found in Péniguel and Rupp (1994a, 1994b).

The convection part

Again the purpose of this article is not to present the fluid codes retained in detail. Basically the average Navier-Stokes equations are solved. Turbulence is taken into account thanks to an eddy viscosity model like a $k-\varepsilon$. The boundary layer is handled through local wall functions. More details can be found in Chabard and Pot (1995); Mattéi and Simonin (1992); Delenne *et al.* (1995).

The radiation part

One will devote more time to present the radiation part. All substances emit electro-magnetic radiation. Unlike convection or conduction, radiative energy is transmitted without need of a medium. A fairly complex radiation exchange occurs inside the enclosure as radiation leaves a surface, travels to other surfaces and is partially reflected, re-reflected many times with partial absorption at each contact with a surface. The general equation is very complex to handle. Fortunately, in many engineering systems calculation of radiant interaction among diffusely emitting and reflecting surfaces can be performed under the assumption that surfaces are gray. This implies that the emissivity ε and the absorptivity are equal (Kirchoff law) (here $\rho = 1-\varepsilon$). If one notes $J(x)$ the rate at which radiant energy streams away from a point x, $E(x)$ the emission at point x, the following continuous equation applies:

$$J(x) = E(x) + \rho(x) \int_{y \in S} J(y) \, \frac{cos\theta_1 \, cos\theta_2}{\pi r^2} \, dy \tag{1}$$

θ_1 and θ_2 are the angles between the normals at location x and y and the line of sight joining these points, r is the distance between point x and y. In order to solve this equation numerically, one has to break down the surface S of the enclosure into a finite number of patches and solve a discrete system of equation for the radiosity of these patches. To further simplify the problem, the assumption is made that values across the surface of each patch are constant.

Let us suppose that the surface of the enclosure is subdivided into a collection of N disjoint patches having a surface noted A_i. In the present development all patches (noted P_i) are constituted of planar triangle surfaces with straight edges. Equation (1) becomes:

$$J(x) = E(x) + \rho(x) \sum_{i=1}^{N} \int_{y \in P_i} J_i \, \frac{cos\theta_1 \, cos\theta_2}{\pi r^2} \, dy \tag{2}$$

J_i is the uniform radiosity of patch i, it can therefore be moved outside the integral. Moreover, if one introduces:

$$J_i = \frac{1}{A_i}\int_{x\in P_i} J(x)\,dx \quad \text{and} \quad E_i = \frac{1}{A_i}\int_{x\in P_i} E(x)dx \tag{3}$$

equation (2) becomes:

$$J_i = E_i + \rho_i \sum_{j=1}^{N} J_j \frac{1}{A_i}\int_{x\in P_i}\int_{y\in P_j} \frac{cos\theta_1\, cos\theta_2}{\pi r^2} dydx \tag{4}$$

One purely geometrical quantity appears in equation (4): the view factor (or form factor) F_{ij}

$$F_{ij} = \frac{1}{A_i}\int_{x\in P_i}\int_{y\in P_j} \frac{cos\theta_1\, cos\theta_2}{\pi r^2}\ dydx \tag{5}$$

F_{ij} can be interpreted physically like the proportion of the total power leaving patch P_j that is received by patch P_i. It has numerous properties of interest (reciprocity or additivity for example) when calculating and storing the view factors.

Calculation of the view factors

Numerous techniques exist for the calculation of view factors (contour integration, projection methods like Nusseltsphere or hemicube, Monte-Carlo). Choosing an appropriate one is important, indeed the computation of the N^2 view factors (for an enclosure subdivided in N independent patches) is often considered as a fairly costly process.

2D Cartesian and 3D view factors

The 2D Cartesian case degenerates to an elementary expression (Hottel's crossed string method) when the couple of patches is fully visible. For 3D cases, a method based on contour integrals (see Siegel and Howell, 1981) has been used (see Figure 1). Using Stokes theorem, the order of integration can be reduced from four to two, and the view factor expression becomes:

$$F_{ij} = \frac{1}{2S_i\pi}\int_{C_i}\int_{C_j} \log r\ dr_i\ dr_j$$

A special treatment is required for cases where singularities appear in the integrand. This is typically the case when two patches are in contact. The distance r vanishes to 0, therefore the integrand goes to infinity. However, it is also clear that the integral is bounded. After some fairly tedious manipulation, it can be shown that all cases leading to non definite integrand have a closed analytical integral solution. This analytical solution has been implemented in SYRTHES. In other configurations, the integral can be reworked and partially

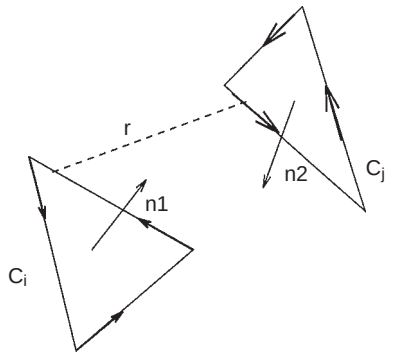

Figure 1.
Contour integrals

analytically integrated. This methodology has the advantage that the integrand of remaining part to integrate behaves smoothly and can be integrated numerically at low cost. This provides a very efficient method both in terms of accuracy and computing cost. Two examples will illustrate the type of test cases performed to check the implementation, see Lin and Sparrow (1965) for the analytical formula (Figures 2 and 3, Tables I and II).

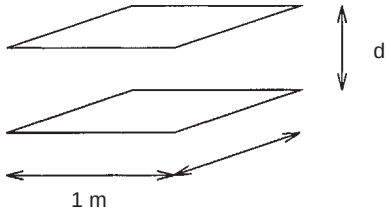

Figure 2.
Rectangular patches facing each other

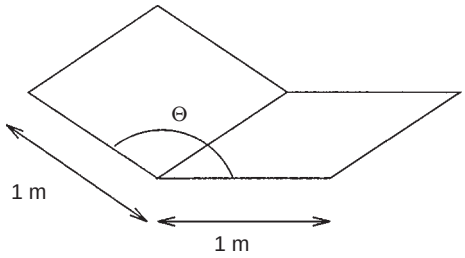

Figure 3.
Rectangular patches forming a corner

$d(m)$	Analytical	SYRTHES
10	0.00316205683	0.00316205683
1	0.19982489569	0.19982489569
0.1	0.82699452239	0.82699452297
0.01	0.98041660292	0.98041660542
0.001	0.99800563190	0.99800606681
0.0001	0.99980007097	0.99980026059

Table I.
Rectangular patches facing each other

Handling the occlusion cases

The shadowing aspects still need to be addressed. A ray-tracing method has been used to overcome this particularly difficult problem. After using low cost tests based on normals, coordinates, etc. to eliminate easy cases and reduce as much as possible the number of costly tests, one draws rays between each vertex of the couple of patches. SYRTHES checks if occluding patches intersect the rays. If no intersection is found, the standard computation of form factor can be performed, otherwise it means that a partial shadowing is taking place. An option is then available, to subdivide the two initial patches in sub-patches, and computations are carried out on each pair of sub-patches. Then additivity rules apply for each sub-patch leading to the global F_{ij}. The depth of refinement is chosen by users and is basically a tradeoff between accuracy and cost.

Testing all patches likely to intersect would be very costly, therefore an efficient algorithm has been implemented to handle this task. The principle is exposed on a 2D case, but the same methodology applies in 3D. The first step consists in building a quad-tree (see Figure 4). Space is partitioned in boxes (4 in 2D, and 8 in 3D), and patches are stored in the box they belong to. If the number of patches in one specific box is above a certain level this particular box is split recursively up to the point when each box contains a satisfactory number of patches.

At this stage, we test if a ray between two points (here A and B) is stopped by an intermediate patch (see Figure 5).

The first step is to determine that point A is located in box B_1. Then, one follows the ray to B. The ray goes through box B_1. Then the patches belonging to box B_1 are tested. Since no intersection occurs, the algorithm keeps on going and finds out that the ray is entering into box B_2. Again, the B_2 patches are

Angle θ	Analytical	SYRTHES
30	0.6190283	0.61902831
60	0.3709053	0.37090532
90	0.2000438	0.20004377
120	0.0866150	0.08661500
150	0.0213453	0.02134532
180	0.	0.00000002

Table II.
Rectangular patches forming a corner

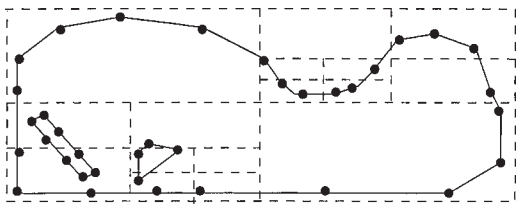

Figure 4.
Building of a quad-tree

tested but now an intersection is found. The conclusion is that point B cannot be seen by A. Compared to the total number of patches, this elementary example shows clearly that the number of patches tested has been dramatically reduced.

The 2D axisymmetrical case

Some industrial problems exhibit an axisymmetrical geometry. Since the conduction code is capable of handling such cases on a bidimensional grid, it was tempting to introduce the possibility of calculating the radiation problem on a 2D grid as well. Indeed, it is much easier to generate a 2D mesh, moreover the number of independent patches (segments in that case) is much lower. The treatment used for the 2D Cartesian case doesn't apply anymore. Another approach has been followed. After some manipulation, an axisymmetrical view factor is expressed as an analytical function with respect to the angle of visibility. Thus the order of integration has been reduced from four to two. The remaining two integrals (corresponding to the integration along each segment i an j) can be integrated with classical numerical methods.

Two rings on a cone (always visible segments)

Very good agreement is found between analytical and calculated view factors, when the segments always see each other (see Figure 6 and Table III). However, in most cases, the determination of the view factor is not trivial. Indeed some patches can see each other at a certain angle and are occluded by intermediate patches at other angles (see Figures 7 and 8).

When occlusion is occurring, a fairly delicate task still needs to be done. It consists in finding out the proper angles of integration (or visibility). The method implemented in SYRTHES, is to check if an intersection occurs between the point i located in plane ($\theta = 0$) and the point j located in a vertical plane forming an angle θ. To achieve this at low cost, a projection of the 3D ray in the polar system of coordinates is used. After elimination of trivial patches (segments), all potential occluding candidates are tested. The accuracy of the method is dependant on the discretization retained. In practice, an angular discretization of 72 sections, or 144 (between $[0, \pi]$) seems adequate to provide

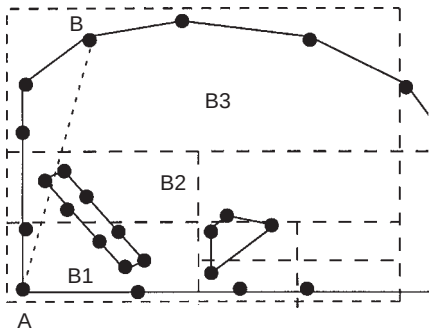

Figure 5.
Visibility test between A and B

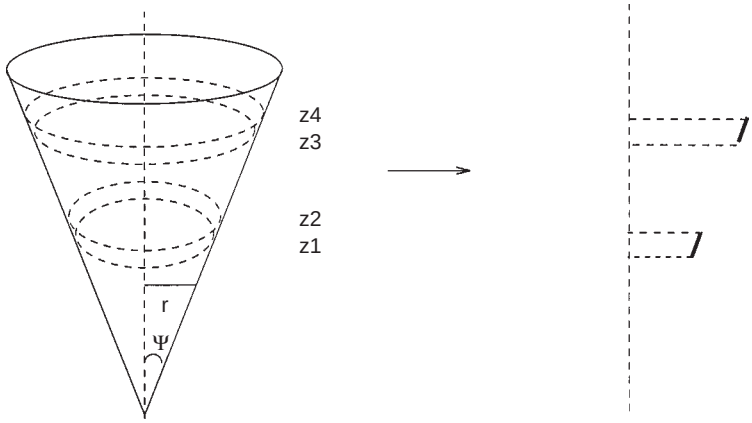

Figure 6.
Segments defining a cone

ψ	z1	z2	z3	z4	Analytical	SYRTHES
$\pi/6$	0.	0.1	0.5	0.6	0.0145100568276	0.014510056830
$\pi/6$	0.	0.1	0.2	0.25	0.0139078991326	0.013907899019
$\pi/4$	0.	0.1	0.5	0.6	0.0260748111926	0.026074811215
$\pi/4$	0.	0.1	0.2	0.25	0.0229771224013	0.022977122422

Table III.
Comparisons for segments on a cone

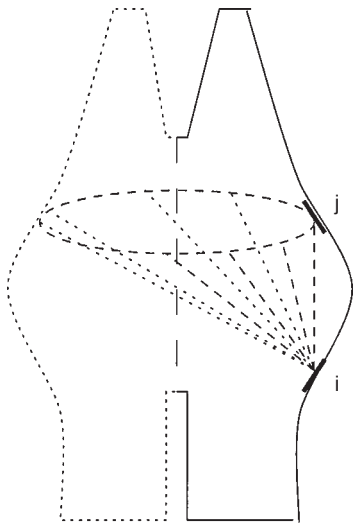

Figure 7.
Definition of an angle of integration (total visibility)

accurate results. The following example (see Figure 9 and Table IV) gives the validation performed on two concentric cylinders, for which an analytical expression is known.

It should be stressed that the method implemented is quite efficient because all the information stored, generated and even the computations are all taking place in a 2D space, even if thermal radiation is treated exactly.

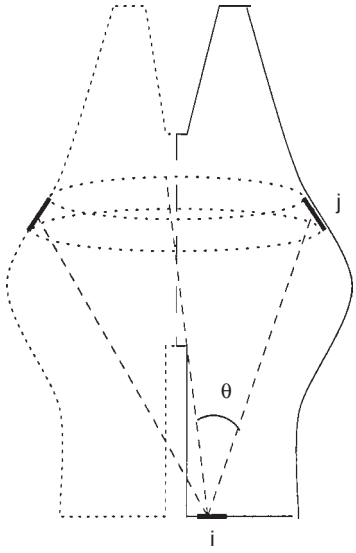

Figure 8.
Definition of an angle of integration (partial visibility)

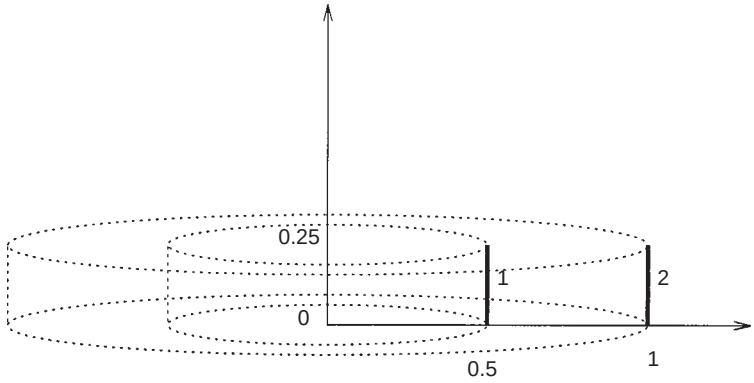

Figure 9.
Validation of an axisymmetrical case with shadowing

Surf x view factor	S_1F_{12}
Analytical	0.21094110
SYRTHES	0.21094158

Table IV.
Validation of an axisymmetrical case with shadowing

Handling symmetries and periodicity

Quite often, when dealing with complex industrial cases, one wants to take opportunity of symmetries or periodicity to reduce the calculation cost. With radiation, one has to overcome the fact that it propagates in the whole domain (even if only one part is modeled). The procedure retained is to duplicate the initial grid up to the point when the radiation grid defines a closed domain. Taking advantage of view factor properties, it is clear that only one part of the

view factors needs to be calculated and stored. Typically, for a collection of N independent patches, with one symmetry, the total number of patches will be 2N, but the number of view factors to compute will be only $N(N+1)$ instead of $N(2N+1)$ and the storage necessary will be $N(N+1)/2$ since the contributions of a patch j and its image through the symmetry j^* to a patch i will be added and stored at the same place in the matrix.

Solving the system

The enclosure being composed of N patches, a system of N linear equations with N unknowns (the radiosity of each independent patch) can be written.

$$\begin{pmatrix} 1-\rho_1 F_{11} & -\rho_1 F_{12} & . & -\rho_1 F_{1N} \\ -\rho_2 F_{21} & 1-\rho_2 F_{22} & . & . \\ . & . & . & . \\ -\rho_N F_{N1} & . & . & 1-\rho_N F_{NN} \end{pmatrix} \begin{pmatrix} J_1 \\ J_2 \\ . \\ J_N \end{pmatrix} = \begin{pmatrix} E_1 \\ E_2 \\ . \\ E_N \end{pmatrix} \quad (6)$$

An iterative conjugate residual method is used to solve the system. It converges in a few iterations due to the property of the matrix. Such a system is written and solved for each wavelength band when the radiative properties of the wall vary according the wavelength. In that case the exitance for each system $E_i[\lambda, \lambda + \Delta\lambda]$ corresponds to the integral of the Planck spectrum over the specific band $[\lambda, \lambda + \Delta\lambda]$ instead of $\varepsilon\sigma T^4$ when the material behaves as a gray body.

Algorithm to couple conduction radiation and convection

Let T_s be the temperature of an internal solid node, T_w the temperature at a node which belongs to the interface, and T_f the temperature of a fluid point (located generally in the log layer) and P_i a radiation patch (see Figure 10).

At time t^n, T_s^n, T_w^n, T_f^n are known

- From the local fluid conditions and the wall temperature, the CFD code provides after calculation:

  h_f^{n+1} : the local heat exchange coefficient at time t^{n+1}

  T_f^{n+1} : the local inside fluid temperature at time t^{n+1}

- From T_w it is possible after interpolation to calculate an average temperature T_i for each radiation patch P_i, from which emittance is computed. Once solved the radiosity system yields the radiative flux to apply on the solid boundary.

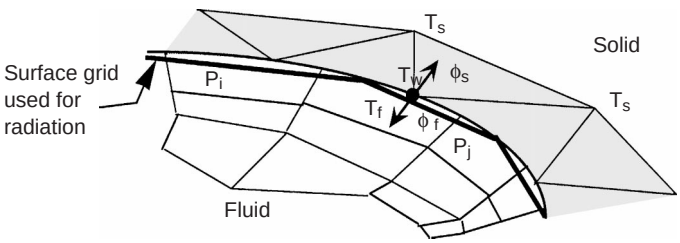

Figure 10.
Data exchange

$Flux_{rad} = h_{rad}^{n+1}\left(T_w^{n+1} - T_{rad}^{aux}\right)$ with $T_{rad}^{aux} = \left(\frac{1}{\sigma}\sum_{j=1}^{N} F_{ij}J_j\right)^{1/4}$
and $h_{rad}^{n+1} = \varepsilon_i\sigma\left(\left(T_w^n\right)^2 + \left(T_{rad}^{aux}\right)^2\right)\left(T_w^n + T_{rad}^{aux}\right)$
ε_i being the emissivity and J_i the radiosity of patch i. F_{ij} is the view factor between patch i and j.

- After interpolation on the solid grid (T_{rad}^{aux} becomes T_{rad}^{n+1}), the flux to be applied is

$$\phi_s^{n+1} = h_f^{n+1}\left(T_w^{n+1} - T_f^{n+1}\right) + h_{rad}^{n+1}\left(T_w^{n+1} - T_{rad}^{n+1}\right)$$

  The notation T_w^{n+1} indicates that this temperature is treated an implicit way.

- Using this flux (or exchange conditions (h, T)) the heat conduction equation gives updated values of T_s^{n+1} over all the solid domain (and of course on the interface where they are noted T_w^{n+1}).

Thus T_s^{n+1}, T_w^{n+1}, T_f^{n+1} are known at time t^{n+1}

Details on the calculation of the turbulent heat exchange coefficient h_f are given in Delenne and Pot (1995) and Péniguel and Rupp (1993). Details on the radiation system solved can be found in Péniguel and Rupp (1995).

The difficulty originating from the non-linearity in temperature has been removed by linearization of the boundary condition. Then this condition is treated implicitly by the conduction code. No stability problem has been observed so far.

To remove the big problem of memory required for the storage of view factors, one relies on an independent surface grid provided by users. This allows the number of triangular independent patches to stay reasonable (less than 5,000 for example) with a grid refinement located exactly where users wish it to be. Of course, this implies at each step to interpolate quantities between the conduction grid and the radiation grid. This interpolation is performed automatically by SYRTHES.

Applications

A 3D case

The 3D problem treated corresponds to the warming of metal plates (10cm thick) of arbitrary shape placed in an oven. The main dimensions of this "oven" are indicated on Figure 11. One considers here that the oven is heated by the top. This condition is modeled by setting the external top side of the wall at a fixed temperature of 1200°C. The external wall of the oven on the side and the bottom is maintained at a cold temperature of 20°C. Only 1/6th of the geometry has been modeled (see Figure 11 and Figure 12), however by periodicity (six times here) the full domain forms a closed enclosure. The conduction grid contains 13,608 elements and 23,510 nodes.

The radiation grid is composed by 2,300 independent patches.

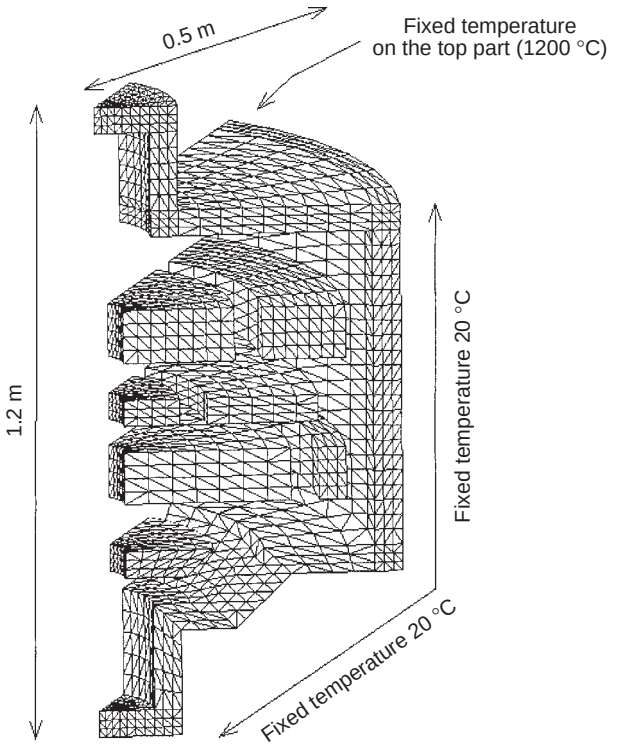

Figure 11.
Conduction grid

As explained earlier, the number of calculated view factors is not $(6.2300)^2/2$ but only $6.(2300).(2301)/2$, and the number of view factor stored is $(2300).(2301)/2$. A time step of 100 seconds has been retained. By radiation the inner plates successively warm up. No stability difficulties have been encountered during the transient before reaching a steady state (see Figures 14 and 15). Figure 13 presents the thermal transient observed.

The CPU time, on a SKI workstation, required for the initialization (including the view factors calculation) is 2,945s. Each radiation system costs around 3.7s to solve, while a conduction step costs around 8.9 seconds.

A 2D axisymmetrical case

The second example given is fairly similar to the previous one but is treated with the axisymmetrical option. Figure 16 presents the conduction and radiation grids. The grid size is 586 elements and 1,393 nodes for the conduction grid and 96 independent segments for the radiation grid. The initialization takes 0.99s (including the calculation of the view factors) on a SGI workstation, and each time step of 100s is performed in less than 0.05s (0.042s for the conduction, and 0.0038s for the radiation).

Figure 17 presents the temperature contours during the transient. The same behavior as for the 3D case is observed.

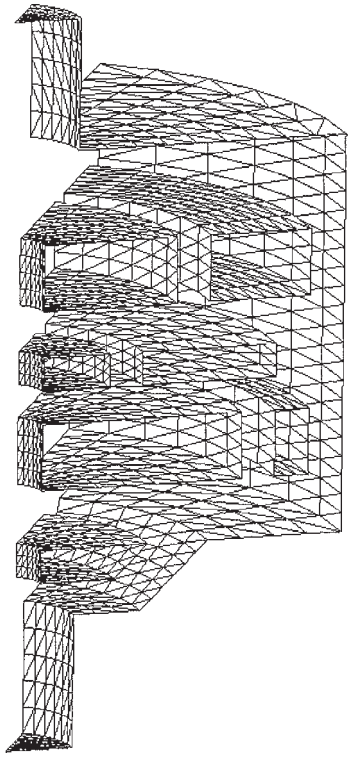

Figure 12.
Radiation grid

Coupling convection conduction and radiation

The example given concerns underground electrical cables. To meet environmental requirements, EDF is planning to rely more and more on underground cables to transport electricity. Independently of the financial aspect, one has to make sure that such an option is technically possible from the thermal point of view. Indeed, by Joule effect, the inner cable tends to warm up. The heat released increases with temperature. Above a certain critical

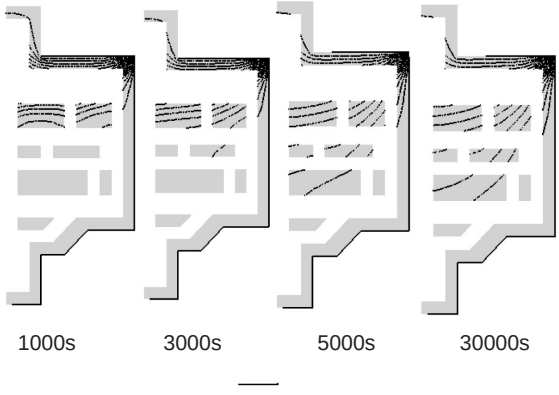

Figure 13.
Thermal contours in a section

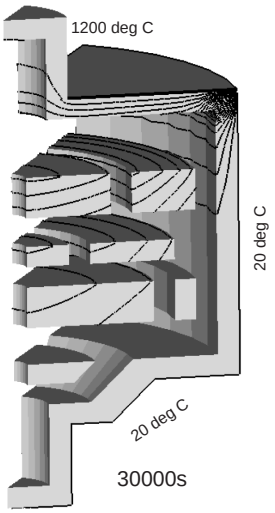

Figure 14.
Thermal contours once the steady state reached

temperature, damage can arise. In reality, heat is transmitted through the earth, and an equilibrium is reached.

Here in this simplified configuration, the outer side of the envelop is maintained at a low temperature of 20°C. The Joule effect is simulated by a constant source term whose value is $35326.64 W/m^3$. Thanks to the very long pipe geometry, the 2D approximation is justified as long as the cable is perfectly horizontal. For the radiation, the 2D Cartesian option is activated. Initially at 20°C, the thermal transient is simulated and a permanent state is obtained after a few hours. The fluid Cartesian grid (58x117) is used by the finite volume CFD code ESTET. The solid grid used by SYRTHES, contains

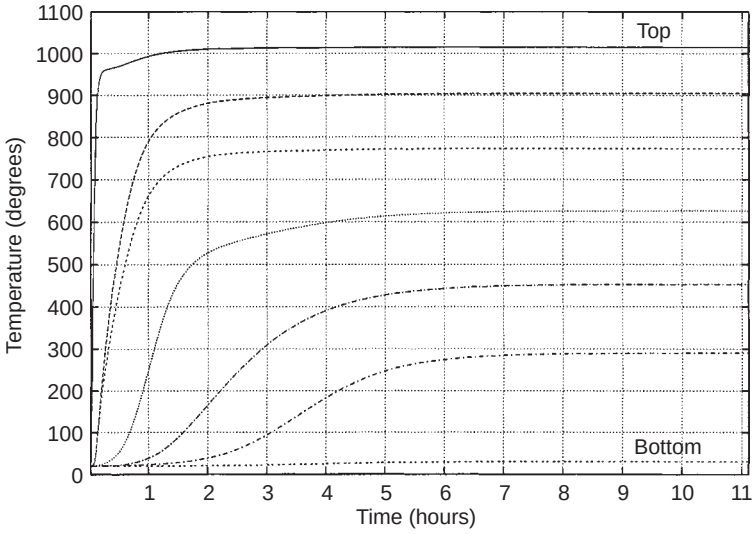

Figure 15.
Temperature evolution of the plates (bottom and top)

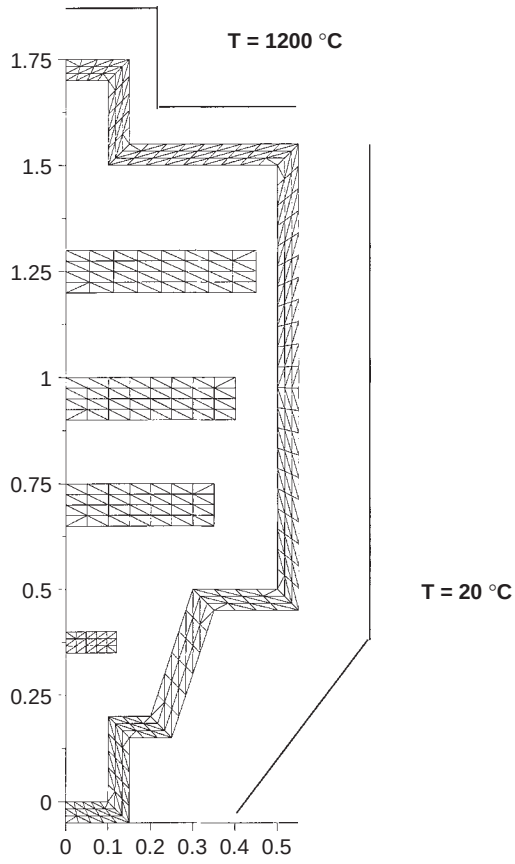

Figure 16.
Grid used for the 2D axisymmetrical example

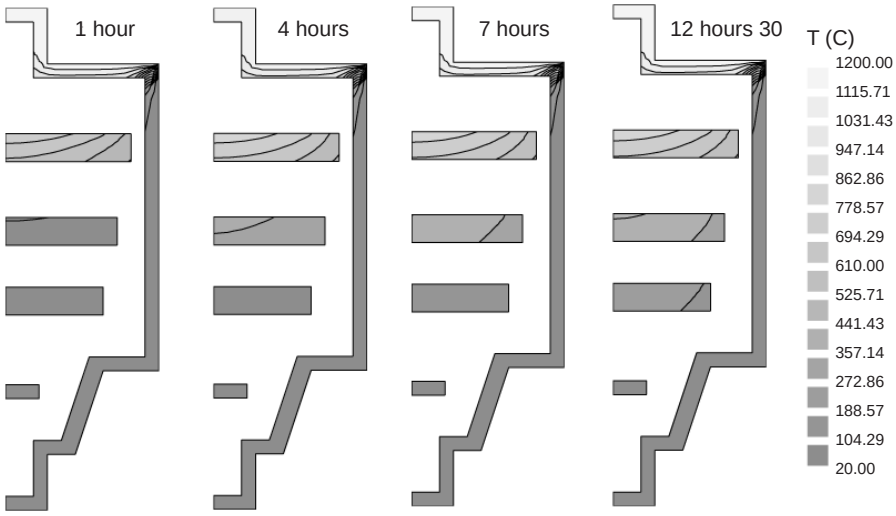

Figure 17.
Thermal contours during the transient

2,408 nodes (Figure 18). It is clear that nodes are not coincident at the interface even if they approach the same geometrical boundary. This provides a very appreciated flexibility for industrial configurations.

Figures 19 and 20 present the thermal field and the velocity field once a steady solution has been obtained. A free convection loop is taking place due to the differential temperature existing between the inner cable and the external pipe. It is interesting to notice the influence of each phenomena, taken separately, which is easy to do by calculation. It appears that even at these relatively low temperatures almost 80 per cent of the energy transfer is taking place by radiation, which is coherent with experimental measurements, and simplified approaches.

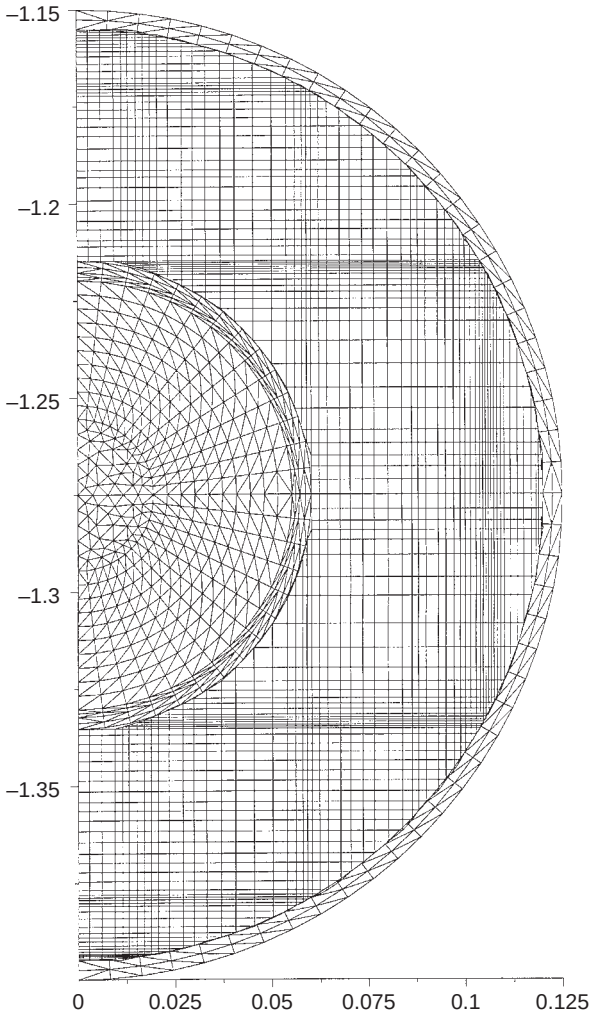

Figure 18.
Grid used by ESTET and SYRTHES

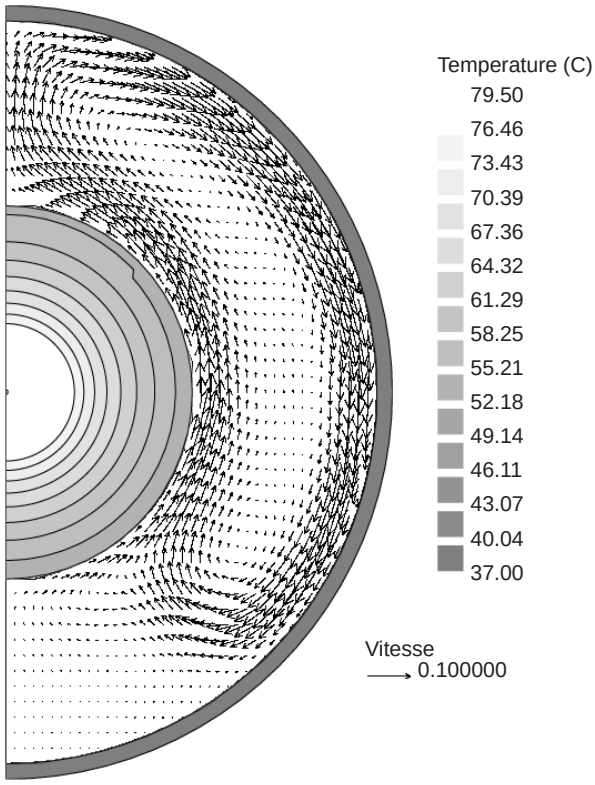

Figure 19.
Velocity and temperature

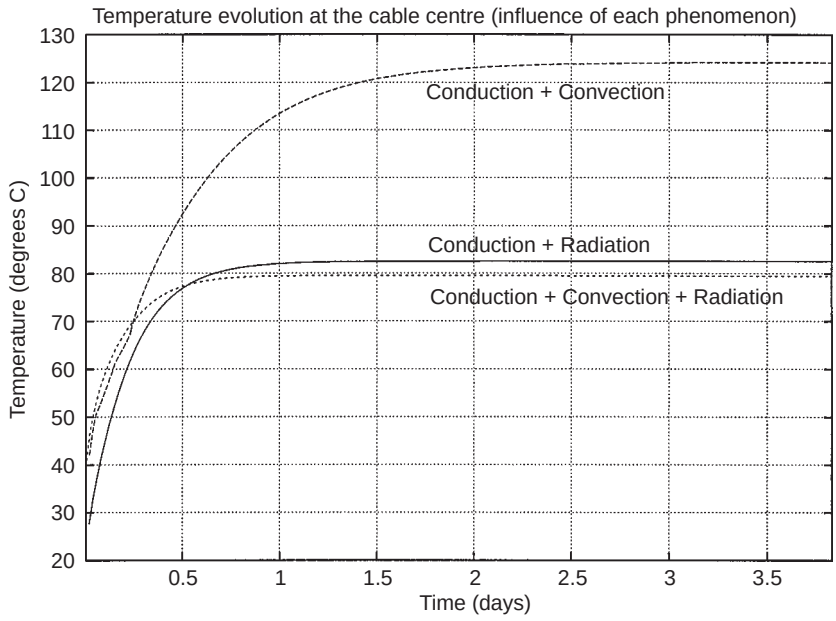

Figure 20.
Temperature evolution

Conclusion

This paper has presented a numerical approach to simulate complex thermal problems where radiation, convection and conduction are present. Neglecting one of these modes may lead to bad prediction. Accurate and efficient algorithms to calculate the view factors have been implemented. Using independent grids for conduction and radiation and convection provides an attractive flexibility, moreover it makes sure that the number of patches used for radiation stays reasonable and that refinement takes place where it is most needed. The cost increase compared to a purely conductive or convective study stays very reasonable. It is worth noting that SYRTHES can also be coupled to several CFD codes simultaneously thanks to message passing techniques (see Péniguel and Rupp, 1997) leading to an interesting numerical tool when conduction, radiation and convection are simultaneously present.

References

Chabard, J.P. and Pot, G. (1995), "Turbulence modelling in finite element industrial applications", *Finite Element in Fluids – New Trends and Applications*, Venezia, pp. 775-84.

Delenne, B., Manzonni, D. and Pot, G. (1995), "Turbulent thermal boundary layer implemented in CFD code N3S and application to flows in heated rooms", *International Journal for Numerical Methods in Fluids*, Vol. 20, pp. 469-592.

Lin, S.H. and Sparrow, E.M. (1965), "Radiant interchange among curved specularly reflecting surfaces. Application to cylindrical and conical cavities", *Trans ASME J. Heat Transfer*, Vol. 87 No. 2, pp. 299-307.

Mattéi, J.D. and Simonin, O. (1992), "Manuel théorique du code ESTET version 3.1 Modélisations physiques", Internal report EDF.

Péniguel, C. and Rupp, I. (1993), "A numerical method for thermally coupled fluid and solid problems", *Numerical Methods in Thermal Problems*, Swansea, pp. 1027-39.

Péniguel, C. and Rupp, I. (1994a), "A finite element approach to simulate general conduction problems", *3rd Int Conference Heat Transfer*, Southampton, pp. 555-62.

Péniguel, C. and Rupp, I. (1994b), "A numerical approach for thermally coupled fluid and solid problems in complex geometries", *3rd Int Conference Heat Transfert*, Southampton, pp. 27-34.

Péniguel, C. and Rupp, I. (1995), "A numerical approach of coupled heat conduction and enclosure radiation problems", *Finite Element in Fluids – New Trends and Applications*, Venezia, pp. 787-96.

Péniguel, C. and Rupp, I. (1997), "Coupling conduction radiation and convection using PVM", Ecole Nationale des Ponts et Chaussées, St Venant Symp., Paris, pp. 237-44.

Siegel, R. and Howell, J.R. (1981), *Thermal Radiation Heat Transfer*, 2nd ed., Hemisphere Publishing Corporation, New York, NY.